Fermilab FERMILAB-Conf-01/149 July 2001

FIELD QUALITY OF THE FERMILAB Nb_3Sn HIGH FIELD DIPOLE MODEL*

N. Andreev, D. Chichili, C. Christensen, J. DiMarco, V.V. Kashikhin, P. Schlabach†, C. Sylvester, I. Terechkine, J.C. Tompkins, G. Velev, A.V. Zlobin, FNAL, Batavia, IL 60510, USA

Abstract

A short Nb_3Sn dipole model based on a single-bore cos-theta coil with a cold iron yoke has been fabricated and tested recently at Fermilab. Field quality was measured at room temperature during magnet fabrication and at helium temperature. This paper reports the results of cold magnetic measurements. The geometrical harmonics, the coil magnetization effect caused by persistent currents in superconductor and eddy current in the cable, the "snap-back" effect at injection are presented and compared with theoretical predictions.

1 INTRODUCTION

High field accelerator magnets are being developed at Fermilab for next generation hadron colliders. These magnets are designed for a nominal field of 10-12 T in the magnet bore of 40-50 mm at the operating temperature of 4.3 K and are based on different design approaches and fabrication techniques [1,2]. To achieve these design parameters Nb_3Sn superconductor is used. One of the design approaches being explored for these magnets is based on the cos-theta coil.

A model magnet program to validate and optimize the magnet design has been undertaken. A 1 m long model magnet (HDFA02) was recently fabricated and is being tested in the Fermilab Vertical Magnet Test Facility. During this test magnetic measurements were performed both warm and cold. Cold measurements were made at excitation currents up to 7 kA before quench training.

2 MAGNET DESIGN

Magnetic design and parameters of the short model are reported in [3].

The design of the HFM consists of two layer shell-type coil with a 43 mm bore and cold iron yoke. Fig. 1 is a 3d view of the magnet. The magnet utilizes a keystoned Rutherford-type cable made of 28 Nb_3Sn strands, each 1 mm in diameter. The strands were manufactured using the Modified Jelly Roll (MJR) process. Both inner and outer layers of the coil are made from the same cable. The cable has a 25 μm thick stainless steel core in order to control crossover resistance. A 0.125 mm thick ceramic tape impregnated with liquid ceramic binder is used for cable insulation. The critical current for the virgin strand measured at 12 T, 4.2 K was 726 A and extracted strand 665 A. The critical current degradation in the magnet is 8.5%. Strand and cable RRR was within a range of 7-19.

*Work supported by the U.S. Department of Energy
†schlabach@fnal.gov

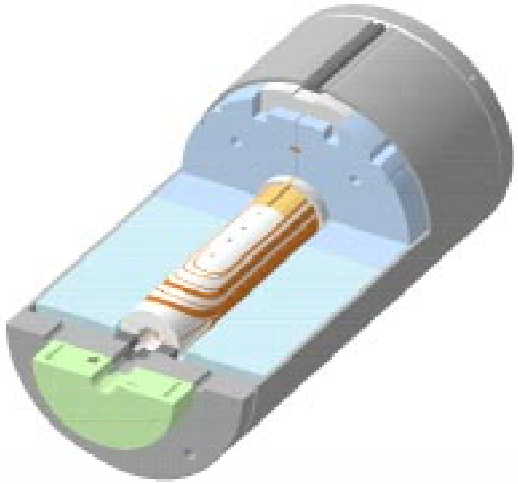

Figure 1: Two-layer shell-type Nb3Sn dipole model

Each half-coil consists of 24 turns, 11 turns in the inner layer and 13 turns in the outer layer. Two pole posts, one in the inner layer and another one in the outer layer, and four spacers per quadrant, two for each layer, minimize the low order geometrical harmonics in the magnet body. The coil ends have also a blockwise layout of turns with the same number of blocks and turns in the block as in magnet body. The design goals for the magnet end optimization were stress minimization in the cable blocks and minimization of the end length to increase the magnet straight section for a fixed total coil length.

The iron yoke has an inner diameter of 120 mm and an outer diameter of 400 mm. No special holes for compensation of the iron saturation effect were used in this model. The optimized iron yoke will be used in the next short model.

Magnet technology and the details of the short model fabrication are reported elsewhere [4].

3 MEASUREMENT SYSTEM

Magnetic measurements presented in this paper were performed using a vertical drive, rotating coil system utilizing a coil of 2.5 cm nominal diameter and 25 cm length. It has a tangential winding for measurement of harmonics as well as dedicated dipole windings measuring the lowest order component of the field and allowing for bucking the large dipole component in the main coil signal. Coil winding voltages as well as magnet current are read using HP3458 DVMs. DVMs are triggered simultaneously by an angular encoder on the probe shaft, synchronizing measurements of field and current. A centering correction is performed using feed

down of higher order allowed to lower order unallowed harmonics (18, 22 pole to 16, 20 pole).

4 FIELD QUALITY ANALYSIS

In the straight section of the magnet, the field is represented in terms of harmonic coefficients defined by the power series expansion

$$B_y + iB_x = B_1 \times 10^{-4} \sum_{n=1}^{\infty} (b_n + ia_n) \left(\frac{x+iy}{r_0} \right)^{n-1},$$

where B_x and B_y are the transverse field components, B_1 is the dipole field strength, b_n and a_n are the 2*n*-pole coefficients $b_1=10^4$) at a reference radius r_0 of 10 mm. A rectangular coordinate system is defined with the z axis at the center of the magnet aperture and pointing from the return end towards the lead end, the x axis horizontal and pointing to the right of an observer who faces the magnet from the lead end, the y axis pointing upwards.

4.1 Harmonics in the magnet body

Magnet strength measured in the straight section (0.6154 T/kA, warm, 10 A) agrees well with that expected from the design (0.6140 T/kA). The measured magnetic length of 0.803±0.005m is also in agreement with the calculated value of 0.809 m. A comparison of harmonics measurements at 3 kA (average of up and down ramp) in the magnet body and values calculated for the design geometry is presented in Table 1. In addition we present harmonics that would be produced by the mid plane shifts shown in Fig. 2 which are consistent with the known left right and up down asymmetry in the coil assembly introduced during reaction and coil yoking.

Table 1: Harmonics in the magnet straight section

	Measured		**design values**	**as built**	
n	$\mathbf{A_n}$	$\mathbf{b_n}$	$\mathbf{b_n}$	$\mathbf{a_n}$	$\mathbf{b_n}$
2	-9.6	4.1	-	-9.37	4.23
3	-0.2	-4.0	0.00	-0.02	-3.86
4	-1.1	0.4	-	0.53	0.29
5	0.3	0.0	0.00	0.00	-0.13
6	0.3	0.0	-	-0.07	0.03
7	-0.1	0.1	0.00	0.00	0.05
8	-0.2	-	-	0.02	0.00
9	-0.2	-0.2	-0.09	0.00	-0.09

The residual difference between measured harmonics and those calculated for a plausible as-built geometry are to a large extent consistent with a 50 μm RMS error in block placement (Table 2). Discrepancies in higher order harmonics may be due to the small signal size of this probe, small residual magnetization of the anticryostat or nonlinearity of field harmonics with current.

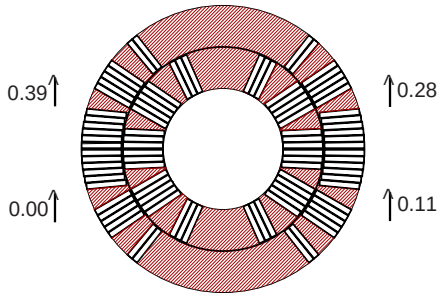

Figure 2: Mid-plane shifts in each quadrant which reproduce the measured low order field harmonics

Table 2: Comparison of residual field differences to effect of block mispositioning

	measured-as built		**50μ RMS block error**	
n	$\Delta\mathbf{a_n}$	$\Delta\mathbf{b_n}$	$\Delta\mathbf{a_n}$	$\Delta\mathbf{b_n}$
2	-0.2	-0.1	-0.19	-0.13
3	-0.2	-0.1	-0.22	-0.14
4	-1.7	0.1	-1.68	0.14
5	0.3	0.1	0.26	0.12
6	0.4	0.0	0.36	-0.01
7	-0.1	0.1	-0.07	0.10
8	-0.2	-	-0.23	-
9	-0.2	-0.1	-0.17	-0.11

4.2 Coil Magnetization

The effect of coil magnetization on measured harmonics in this magnet is large. For example, the width of the b_3 hysteresis curve is 50 units at 1 kA (Fig. 3). This is due to the high J_c and large effective filament diameter that reaches ~100 microns in Nb_3Sn strands produced using MJR or IT (Internal Tin) processes [5]. Calculations of the magnetization harmonics reproduce measure values over a wide range of current as shown in Fig. 4 and 5 for the normal sextuple and decapole.

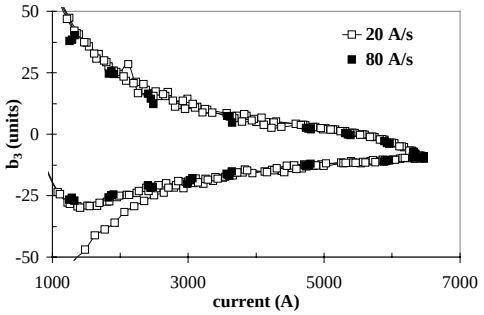

Figure 3: Measured b_3 at different ramp rates

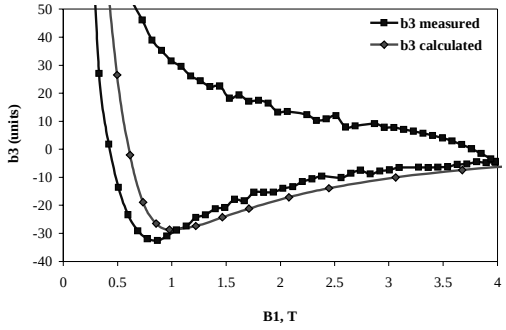

Figure 4: Comparison of measured and calculated b_3

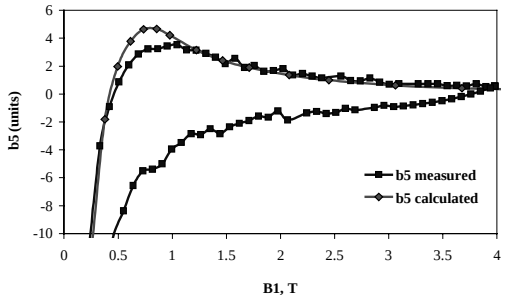

Figure 5: Comparison of measured and calculated b_5

To check for dynamic effects during injection, measurements were performed during a 30 min ‘‘injection” plateau at 3 kA. The plateau was proceeded by 2 standardization cycles in which the magnet was ramped 0-6500-0 A at a ramp rate of 40 A/s. After a 30 minute plateau at 3 kA, current was increased to 4.5 kA with ramp rate of 10 A/s and then ramped down at 40 A/s. Normal sextupole measurements during this cycle are presented in Fig. 6. Fig. 7 shows the first two allowed harmonics during injection and as the magnet is ramped at the end of the plateau. Change in the harmonics during injection is very small with respect to those observed in NbTi accelerator magnets [7]. This is not yet understood and will be studied further in this and future model magnets.

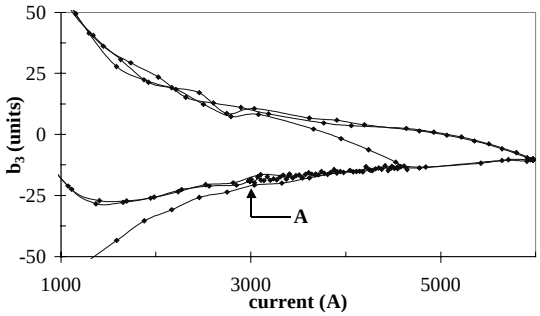

Figure 6: b_3 measured during an accelerator cycle

4.3 Cable eddy currents

Nb_3Sn magnets have typically had large eddy current harmonics due to the small crossover resistance created during coil reaction [6]. To control crossover resistance, cable in this magnet has a 25 μm stainless steel core. It can be seen from the agreement between the hysteresis width of harmonics measurements at 20 and 80 A/s (Fig. 3) that eddy currents in this model are small.

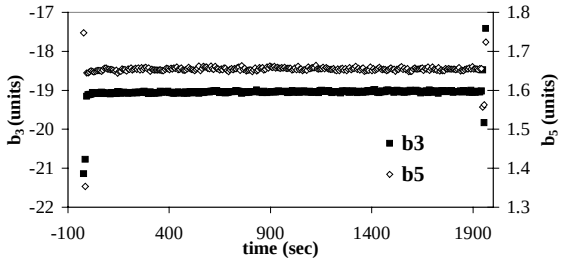

Figure 7: b_3, b_5 near the injection plateau

5 CONCLUSIONS

Field measurements from tests before quench training of a model dipole magnet in the Fermilab high field magnet program are consistent with expectations. Body harmonics are consistent with a plausible model of the as-built geometry. The relatively large measured magnetization harmonics are consistent with calculations A scheme to correct this with passive correction shims will be tested in further tests of this model. The pronounced decay and snapback effect seen in NbTi magnets at injection has not been observed. A stainless steel core in the cable has apparently eliminated large eddy current harmonics seen in other Nb_3Sn magnets. Further tests of this model will be performed and additional models in this design series are expected before the end of this year.

6 REFERENCES

[1] A. Zlobin et al., “Development of Cos-theta Nb_3Sn Dipole Magnets for VLHC”, this conference.

[2] Y. Terechkine et al., “Development of a Cos-theta Nb_3Sn Dipole Model at Fermilab”, this conference.

[3] G. Ambrosio et al., “Magnetic Design of the Fermilab 11 T Nb_3Sn Short Dipole Model”, IEEE Trans. Appl. Supercond., Vol. 10, No. 1, March 2000, p. 322.

[4] D.R. Chichili et al., “Fabrication of the Shell-Type Nb_3Sn Dipole Model at Fermilab”, IEEE Trans. Appl. Supercond., Vol. 11, No. 1, March 2001, p. 2160.

[5] E. Barzi et al., “Study of Nb_3Sn Strands for Fermilab’s High Field Dipole Models”, IEEE Trans. Appl. Supercond., Vol. 11, No. 1, March 2001, p. 3595.

[6] A. den Ouden et al., “Application of Nb_3Sn Superconductors in High-field Accelerator Magnets”, IEEE Trans. on Applied Superconductivity, Vol. 7, No. 2, June 1997, p. 733.

[7] L. Bottura et al., “Performance of the LHC Final Design Full Scale Superconducting Dipole Prototypes”, IEEE Trans. Appl. Supercond., Vol. 11, No. 1, March 2001, p. 1554.